Modulated Photophysics of 3-Pyrazolyl-2-pyrazoline Derivative Entrapped in Micellar Assembly

Paltu Banerjee, Smritimoy Pramanik, Arindam Sarkar, and Subhash Chandra Bhattacharya*

Department of Chemistry, Jadavpur University, Kolkata 700032, India

Received: January 9, 2008; Revised Manuscript Received: February 22, 2008

The photophysical behavior of 3-pyrazolyl-2-pyrazoline derivative (PZ), a newly synthesized biologically active compound has been studied in micellar solutions of anionic sodium dodecyl sulfate (SDS), cationic cetyl trimethylammonium bromide (CTAB) and nonionic *p-tert*-octylphenoxy polyoxyethanol (Triton X-100, TX-100) micelle using steady state and time-resolved fluorescence spectroscopy technique. Influence of the micelles on the photophysics of PZ has also been investigated using different approaches. The location of the fluorophore PZ in the micelle has been identified by cetyl pyridinium chloride (CpCl) induced fluorescence quenching and micropolarity surrounding that fluorophore in micellar solution. The effect of urea on the steady state fluorescence and relaxation dynamics of the micelle bound probe has also been observed. The results have been interpreted in terms of the model that urea displaces water molecules from the micellar interface and the consequent destabilization leads to the expulsion of the probe molecules from the interfacial region. An attempt has been made to determine probe sensing microviscosities for these micellar microenvironments in the light of average reorientation times of the probe PZ.

Introduction

2-Pyrazoline derivatives constitute a class of compounds of pharmaceutical importance.[1–4] A recent trend to synthesize these types of compounds has been increased for their anti-inflammatory, antidiabetic, anesthetic, analgesic and glutamate transport sensing properties.[5–9] The compound is highly fluorescent due to extended conjugation from 2-pyrazoline ring to pyrazole. The fused norborane ring present at the C(4) and C(5) carbon of 2-pyrazoline ring induces steric congestion in the compound. The steric congestion prohibits free rotation at the C(3) of 2-pyrazoline and C(5) of the pyrazole bond. The interest on the photophysical study of pyrazoline derivatives originates principally from two aspects: the first stems from its novel biological applications in pharmaceuticals, and the second one arises due to presence of electron donors and acceptors at N(1) and C(3) positions, respectively. These contribute intrinsically large molecular hyperpolarizabilities of 2-pyrazoline derivatives, and they have widely been used for whitening textile fibers, plastics and papers.[10,11] Stimulation in synthesis of organic nanoparticles from low molecular weight compound 2-pyrazoline derivative becomes a new insight of research.[12,13] Photorefractivity of a two-dimensional array constructed with 2-pyrazoline nanoparticles have wide uses in applied optical field.[14,15] To some degree, 2-pyrazoline derivatives are considered to be an important organic heterocyclic "transition" material, i.e., a material that shares many properties with conventional semiconductors and insulators like organic molecular crystals (with their large absorption oscillator strengths, polaron assisted conduction, etc).[16] The compound (PZ) may be considered an alternative fluorescent probe compared to other probes due to its highly solvent sensitive strong fluorescence. The concentration dependent dimer formation like other probes such as pyrene has not been observed and the compound may be transformed into organic nanoparticles like other pyrazoline derivatives[12,15] to increase its bioactivity.

Besides this, depending on substitution, 2-pyrazoline derivatives exhibit variation in photoinduced intramolecular and intermolecular charge transfer and electron transfer[17,18] processes. The ground and excited state behaviors of 2-pyrazoline derivatives are also influenced by the surrounding medium.[19]

The solvent dependent radiative transitions and relaxation dynamics of pyrazole substituted 2-pyrazoline (PZ) from the S_1 and S_2 states have been established in our earlier publication.[20] Considerable solvatochromism has also been established; i.e., the steady state fluorescence of PZ in polar aprotic and protic solvents occurs from the S_1 state whereas the transition occurs from both the S_1 and S_2 states in water, ethylene glycol and glycerol. Compared to a single solvent or a homogeneous mixture of solvents, organized assembly of nano dimensions possess many unique properties. The most significant property of an organized assembly in spectroscopy is its ability to stabilize and bind solute molecules that are typically insoluble or sparingly soluble in a pure bulk solvent.[21] Upon binding to the microheterogeneous medium a solute will experience a different environment (micropolarity, microviscosity, etc.) compared to that of the bulk pure solvent.[22] The studies on micellar organization and dynamics assume special significance in light of the fact that the general principle underlying the formation of micelles is common to other related self-organized nano bioassemblies such as reverse micelles, bilayers, liposomes and biological membranes.[23–26] Besides, a micellar bioassembly enhances the solubility of hydrophobic drug molecules.[27,28] Therefore attention has been drawn to micellar effects on the nature, i.e., dual fluorescence of the fluorophore in aqueous media and fates of various photophysical processes.[29,30] The basic objective of such studies is 2-fold: first to see how the microenvironment surrounding the probe alter the photophysical processes and second, to characterize the microenvironment surrounding the fluorophore.

* Corresponding author. E-mail: scbhattacharyya@chemistry.jdvu.ac.in, sbjuchem@yahoo.com. Phone: 033 2414 6223. Fax: 91(033) 24146584.

10.1021/jp800200v CCC: $40.75
Published on Web 05/27/2008

SCHEME 1: Structure of PZ

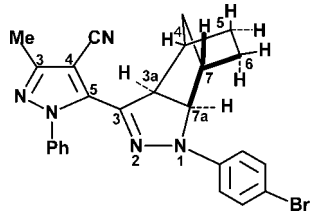

In this present report, the photophysical properties of PZ in microheterogeneous environments, generated by cationic CTAB, anionic SDS and nonionic TX-100 surfactants have been studied. Cetyl pyridinium chloride (CpCl) induced fluorescence quenching experiments of PZ in micelles have been performed to characterize the probable location of the fluorophore PZ. A time-resolved fluorescence study has been used to explore the dynamic quenching of the S_1 state of micellized PZ and investigate how the nature of the micelles (i.e., ionic or nonionic) affects the quenching dynamics. To predict the penetration depth of the PZ in different micelles and the location of the probe in the micelle, the micropolarity surrounding PZ has been determined. The effect of urea on the photophysics of PZ in the micellar medium has also been performed. Variation of lifetime in aqueous micellar medium compared to aqueous medium has also been observed. We are also interested in comparing the rotational relaxation of PZ, which facilitates to determine probe-sensing microviscosity in those microenvironments using average reorientation times.

Experimental Section

The 3-pyrazolyl-2-pyrazoline derivative, 5-((3a*S*,7a*R*)-1-(4-bromophenyl)-3*a*,4,5,6,7,7*a*-hexahydro-1*H*-4,7-methano-indazol-3-yl)-3-methyl-1-phenyl-1*H*-pyrazole-4-carbonitrile (Scheme 1) was synthesized using the method described earlier.[20]

The compound was further vacuum-sublimed before use. The anionic surfactant SDS was purchased from BDH, the cationic surfactant CTAB and the nonionic surfactant TX-100 were procured from Aldrich and were used as received. Analytical grade urea (Merck) and cetyl pyridinium chloride (CpCl) (Lobachemie) were used in this work. The concentration of quencher (CpCl) was kept far below its critical micellar concentration (cmc).

The purified solvent dioxan was found to be free from impurities and was transparent in the spectral region of interest. Triply distilled water was used for the preparation of the experimental solutions.

Absorption spectra were recorded using a Shimadzu UV–vis 1700 spectrophotometer with a matched pair of silica cuvettes. Fluorescence spectra were taken in an F-IIA spetrofluorometer (Spex, Inc.) with an external slit width of 1.25 mm. All measurements were done repeatedly and reproducible results were obtained. All fluorescence spectra were corrected for the instrumental response. Prior to the spectroscopic measurements solutions were deoxygenated by bubbling nitrogen through them. Fluorescence lifetimes were determined from time-resolved intensity decay by the method of time-correlated single-photon counting using a nanosecond diode laser at 403 nm (IBH, picoLED-07) as light source. The typical response time of this laser system was 70 ps. The data stored in a multichannel analyzer was routinely transferred to an IBH DAS-6 decay analysis software. For all the lifetime measurements the fluorescence decay curves were analyzed by biexponential iterative fitting program provided by IBH such as

$$F(t) = \sum_i \alpha_i \exp(-t/\tau_i) \quad (1)$$

α_i is a pre-exponential factor representing the fractional contribution to the time-resolved decay of the component with a lifetime τ_i. Average lifetimes $\langle\tau\rangle$ for biexponential decays of fluorescence were calculated from the decay times and pre-exponential factors using the following equation[31]

$$\langle\tau\rangle = \frac{\alpha_1\tau_1 + \alpha_2\tau_2}{\alpha_1 + \alpha_2} \quad (2)$$

During anisotropy measurements, all transients were taken by using commercially available (IBH) picosecond-resolved time correlated single photon counting (TCSPC) setup (instrument response function (IRF) of ~70 ps). The picosecond excitation pulse from the diode laser was used at 405 nm. The fluorescence from the sample was detected by a photomultiplier after dispersion through a double grating monochromator. For anisotropy decay measurements, emissions at parallel ($I_{||}(t)$) and perpendicular ($I_{\perp}(t)$) polarizations were collected by rotating the analyzer at regular intervals. The time-resolved anisotropy ($r(t)$) was calculated using the following relation:

$$r(t) = [I_{||}(t) - GI_{\perp}(t)]/[I_{||}(t) + 2GI_{\perp}(t)] \quad (3)$$

where G is the grating factor of the emission monochromator of the TCSPC system. All the experiments were performed at ambient temperature (298 K).

Results and Discussion

Absorption Study. The absorption spectrum of an aqueous solution of PZ shows a well-resolved band with maxima at around 396 nm due to a $\pi \rightarrow \pi^*$ transition to the S_1 state. When compared to the homogeneous media provided by organic solvents,[20] the environment of all used micelles does not cause a significant change in the absorption spectrum of PZ (inset of Figure 1b).

Fluorescence Study. Fluorescence techniques have been widely used to characterize micellar organization and dynamics due to their suitable time scale and their noninvasive and intrinsic sensitivity.[32] Therefore the effect of micelles (SDS, CTAB and TX-100) on the fluorescence spectra of PZ has been illustrated in Figure 1.

On gradual addition of SDS, CTAB and TX-100 in aqueous solution of PZ, an enhancement of the fluorescence intensity with minor red shift (in SDS and CTAB) and minor blue shift (in TX-100) of spectral maxima from 496 nm (in aqueous solution) has been observed (Figure 1). Comparing these observations with the polarity of the medium, one can argue that fluorescence of PZ changes with the polarity of the micellar environment. Plots of F/F_0 (where F and F_0 represent the fluorescence intensity of PZ in presence and absence of surfactant) against the concentration of different surfactants make sigmoidal curves. The steep rise points of individual curves, correspond to the critical micellar concentration (CMC) of the surfactants, have been tabulated in Table 1. The CMC values obtained for SDS, CTAB and TX-100 are slightly lower than the CMC values found in the literature.[33,34] Because the CMC of micelles is also dependent on the stereoelectronic nature of the fluorophores, slight variations in the values of CMC obtained with PZ are expected as obtained by others[35] also.

Probe−Micelle Binding Constant. The enhancement of fluorescence intensity of PZ in micellar solution can be rationalized in terms of binding of the probe with the micelle. But the strength of the binding can be identified through the

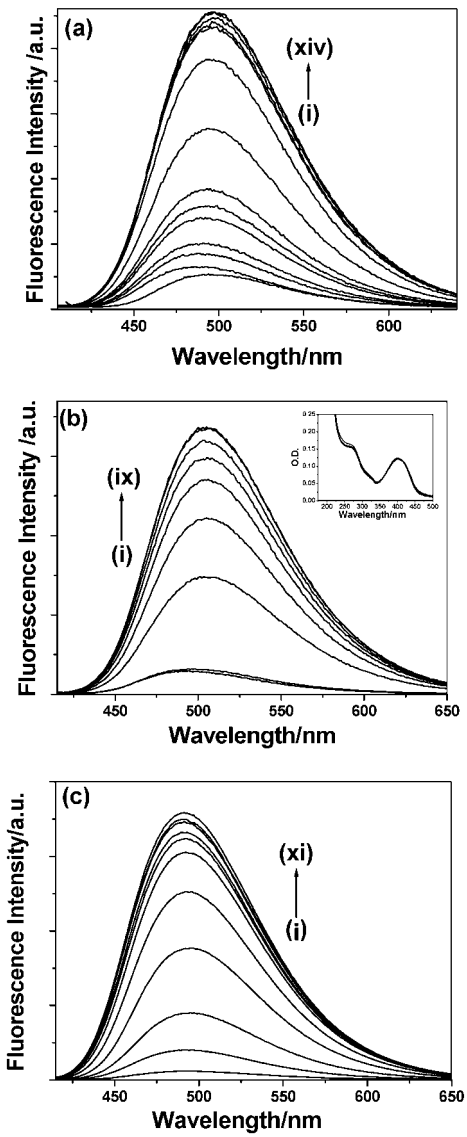

Figure 1. (a) Fluorescence spectra of PZ solution as a function of surfactant concentrations (λ_{exc} = 396 nm). Curves i–xiv corresponds to 0.0, 0.8, 1.2, 1.6, 2.0, 2.4, 3.2, 3.4, 4.8, 5.6, 6.4, 8.7, 9.5, 10.2 m mol dm^{-3} for SDS. (b) Fluorescence spectra of PZ solution as a function of surfactant concentrations (λ_{exc} = 396 nm). Curves i–ix corresponds to 0.0, 0.1, 1.0, 1.2,1.4, 1.6, 1.7, 1.9, 2.1 m mol dm^{-3} for CTAB. Inset: absorption spectra of PZ in aqueous and 1.0, 1.2,1.4, 1.6, 1.7, 1.9, 2.1 m mol dm^{-3} of CTAB. (c) Fluorescence spectra of PZ solution as a function of surfactant concentrations (λ_{exc} = 396 nm). Curves i–xi corresponds to 0.0, 0.06, 0.09, 0.13, 0.20, 0.30, 0.40, 0.60, 0.88, 1.08, 1.27 m mol dm^{-3} for TX-100.

determination of the binding constant between the probe and the micelle. The binding constants between the probe and the micelles have been determined from the fluorescence intensity data following the method described by Almgren et al.[36] According to this method

$$\frac{F_\infty - F_0}{F - F_0} = 1 + \frac{1}{K[\mathrm{M}]} \tag{4}$$

where F_0, F, and F_∞ are the fluorescence intensities of PZ in absence of surfactant, in micellar solutions (micellar concentration [M]), and under conditions of complete micellization respectively. K represents the binding constant between the probe in the excited state and micelle. The micellar concentration [M] has been calculated using the surfactant concentration [S] as [M] = ([S] − CMC)/n, where n is the aggregation number. The aggregation numbers have been taken from the literature.[37,38]

The plot of $(F_\infty - F_0/F - F_0)$ vs 1/[M] in relation to eq 4 (Figure 2) shows the linearity. From the slopes of the individual plots, the binding constants (K) have been determined and the values (Table 1) follow the order of micelles TX-100 > CTAB > SDS.

In nonionic micelle TX-100, the higher binding constant of the probe with micelle may be due to the more stabilization of the probe in the micellar environment compared to other ionic micelles. Due to the very thick palisade layer, most of the fluorescent probes may reside in this layer of the TX-100 micelles where the water structure is not as loose as that in the Stern layer of CTAB and SDS micelles having significantly thinner micellar Stern layer.[39] Compared to that of the Stern layer of CTAB and SDS micelles, PZ experiences a greater microviscosity in TX-100 due to a greater extent of packing of the surfactant chain. The variation of obtained microviscosity values has been discussed in the latter section. Between the two ionic micelles CTAB and SDS, despite the comparable thickness of the Stern layer binding constant of PZ with CTAB is higher than SDS, which may be due to comparatively less hydrated Stern layer for CTAB than SDS, because the headgroup of SDS is hydrated more than the headgroup of CTAB micelle.[40]

CpCl Induced Fluorescence Quenching. To confirm the location of the fluorescence moiety in the micellar environment, we have studied the fluorescence quenching of the probe in the micellar solution using CpCl as a quencher. Quencher with properties similar to the surfactant studied offers important advantages over the more conventional quenchers.[41] In micellar media, fluorescence quenching is influenced by the distribution of fluorophores and quencher species in the micelles.[42] Here the quencher CpCl mixes ideally with the surfactants in the micelles,[41] such as CpCl may enter into the palisade layer or Stern layer and fluorescence quenching occurs. But using other inorganic cationic quenchers, we have been found that no quenching of fluorescence of the probe occurs in cationic micelles of CTAB, which may be due to the repulsive force between the micelle and quencher. Only the surfactant friendly quencher ions are responsible for fruitful quenching under such condition. In that case, hydrophobic interactions are stronger than the electrostatic forces. Fluorescence quenching data are predictable to be useful to rationalize the location of the fluorescence moiety in the interfacial region or core of the micelle. The Stern−Volmer plot for quenching of the S_1 state of PZ by the quencher CpCl in those micellar microenvironments, obtained from the steady state emission spectra are presented in Figure 3.

A linear Stern−Volmer plot was obtained, which can be described using[29]

$$\frac{F_0}{F} = 1 + K_{SV}[\mathrm{Q}] \tag{5}$$

where F_0 and F represent the fluorescence intensities of fully micellized PZ in absence and presence of quencher respectively. [Q] represents the concentration of quencher and K_{SV} is the Stern−Volmer constant. The obtained K_{SV} values in ionic and nonionic micellar environment follow the order TX-100 > CTAB > SDS. From the K_{SV} values (Table 1), the quenching rate constant (k_q) has been calculated using the relation $K_{SV} = k_q\tau$, where τ is the lifetime of the probe in respective micellar microenvironment and the k_q values in ionic and nonionic micelles follow the order TX-100 > CTAB > SDS. The result is in good agreement with the result in the same environment

TABLE 1: Binding Constant of PZ with Different Micelles, Bimolecular Rate Constant (k_q), Stern−Volmer Constant for Quenching of PZ Fluorescence by CpCl, CMC values and Solvent Polarity Parameters (E_T(30)) of Different Micelles

micellar environment	CMC (m mol dm^{-3})	binding constant $\times 10^{-5}$ (mol^{-1} dm^3)	Stern−Volmer constant $\times 10^{-3}$ (mol^{-1} dm^3)	solvent polarity/E_T(30) (kcal mol^{-1})	quenching rate constant (k_q) $\times 10^{-11}$ (mol^{-1}dm^{3}s^{-1})
TX-100	0.25	24.8	2.5	44.0	3.96, 5.52[a]
CTAB	0.70	5.2	2.0	57.6	3.89, 2.05[a]
SDS	6.90	2.5	0.8	60.5	2.00, 1.05[a]

[a] Signifies the quenching rate constant determined from time-resolved study.

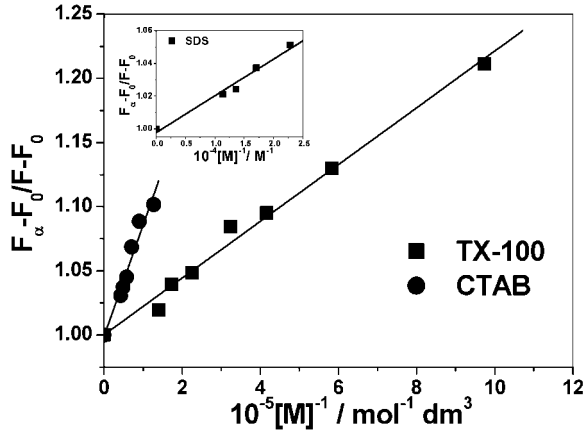

Figure 2. $(F_\infty - F_0/F - F_0)$ vs 1/[M] for TX-100 (●) and for CTAB (●). Inset: plot for SDS; [PZ] = 4.4×10^{-6} mol dm^{-3}.

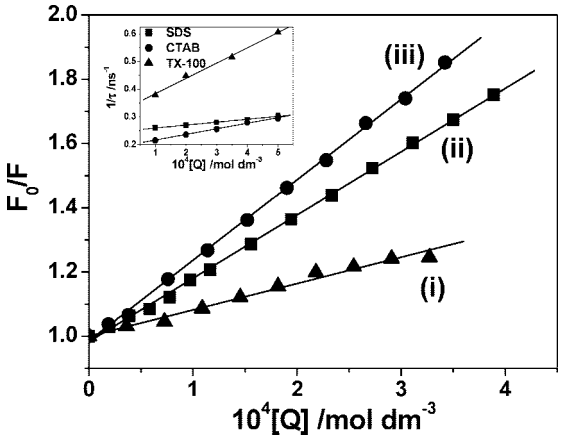

Figure 3. Variation of relative fluorescence intensity (F_0/F) of PZ in (i) SDS, (ii) CTAB, and (iii) TX-100 as a function of the concentration of quencher (Q). Here CpCl was used as a quencher. Inset: $1/\tau$ of PZ in micellar media as a function of the concentration of quencher (Q).

for other probe in our earlier publication.[43] The same results have also been obtained from time-resolved studies, discussed in the last section. The quencher is not supposed to be available in the micellar core because of the very low solubility in that region. It is expected to be available in the aqueous phase as well as in the micellar interfacial region. Hence if the fluorophore be located in the micellar core, there should be no appreciable fluorescence quenching as a result of the lack of availability of the quencher near the fluorophore. However, because the probe is located at the interfacial region then the CpCl induced quenching of the fluorescence occurs in micellar media. The quenching rate constants in micellar media follow the order of the binding constant (Table 1) of the probe with the micelles. The quenching phenomenon is considered to be collisional where the rate is different in different micellar media due to difference in binding strengths of PZ with micelle.

Effect of Urea on Micelle-Bound Probe. The effect of urea on photophysical and/or photochemical processes of probe in different microheterogeneous environments has been studied on the basis of denaturating action of urea towards protein. The alteration of the protein from the disordered state to the native state resembles the micelle (simple replica for more complex biological system) formation. Two mechanisms have been proposed to explain the action of urea. According to the first one, urea acts as a "water structure breaker"[44] and the consequent alteration of water structure leads to greater solvation of hydrocarbon chain. The second mechanism is an indirect one in which urea displaces some of the water molecules from the periphery of microheterogeneous units such as micelle and protein. This phenomenon ultimately modifies the solvation of the fluorophore. Although the first mechanism is a popular one, some recent experimental and theoretical studies[45,46] seem to contradict this. However, the model changes considerably when a hydrophobic group is present. The computer simulation studies[47] show that urea displaces the water molecule in the neighborhood of the hydrophobic group, which is consistent with the second mechanism. Above all controversies, we have studied the effect of urea to the micelle-bound PZ to gain further insight as the micellar size and hydration play a significant role in determining the solvation dynamics and photophysical modulation in micellar media. Addition of urea on the micelle-bound probe (Figure 4) leads to a decrease in the fluorescence yield, suggesting that the fluorophore is expelled from the microheterogeneous environment to the bulk aqueous phase.

The observation in the SDS environment differs from those in other two-micellar media. This suggests that urea can expel the fluorophore from CTAB and TX-100 micelles more efficiently than SDS micelles. There is a scheme that water can enter in the micelles up to a definite depth depending upon the compactness of the micellar units.[48] After addition of urea (8 mol dm^{-3}) fluorescence intensity of SDS bound PZ decreases but remains higher than that in the aqueous media. On the other hand, the fluorescence intensities of the CTAB and TX-100 bound fluorophore in the presence of urea decrease and remain more or less the same as that in the aqueous phase. It can be interpreted that micelles with compact head groups such as SDS experience smaller water penetration compared to the larger headgroup area such as CTAB and TX-100.[49] Using other probe same phenomenon has been reported by Mallick et al.[50] The resulting destabilization of the environment leads to the desolvation of the bound molecule and drives it out to the bulk aqueous phase. From this result one can say that the Stern layer for ionic micelles and palisade layer for nonionic micelle are not hydrated to the same extent.

Micropolarity Surrounding the Fluorophore in Micellar Medium. As the determination of the polarity at probe binding site inside the micelle has great importance in biological systems, attention has been drawn to that direction. A correlation was obtained from the plot of emission maxima (λ_{max}^{em}) of the probe in different composition of dioxan-water mixture against the solvent polarity parameter (E_T(30)). The mentioned parameter

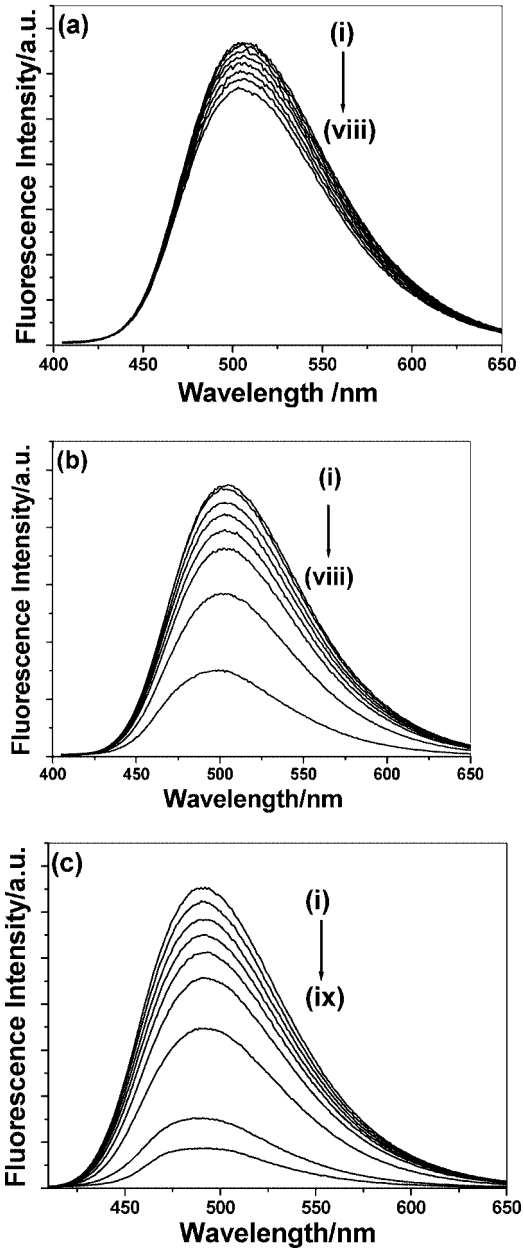

Figure 4. (a) Fluorescence spectra of micelle-bound PZ as a function of added urea in 12 mM SDS solutions ($\lambda_{exc} = 396$ nm). Curves i−viii corresponds to 0.0, 1.0, 1.9, 2.9, 4.9, 5.9, 6.9, 7.9 mol dm^{-3} urea. (b) Fluorescence spectra of micelle-bound PZ as a function of added urea in 3 mM CTAB solutions ($\lambda_{exc} = 396$ nm). Curves i−viii correspond to 0.0, 1.0, 2.2, 3.2, 4.3, 5.3, 6.5, 7.7 mol dm^{-3} urea. (c) Fluorescence spectra of micelle-bound PZ as a function of added urea in 2 mM TX-100 solutions ($\lambda_{exc} = 396$ nm). Curves i−ix correspond to 0.0, 1.0, 2.1, 3.2, 4.3, 5.3, 6.4, 7.5, 8.0 mol dm^{-3} urea.

($E_T(30)$) was developed by Dimorth and Reichardt[51] and based on the transition energy for the solvatochromic intramolecular charge transfer absorption of the betaine dye [2,6-diphenyl-4-(2,4,6 triphenyl-1-pyridino) phenolate]. Resemblance of behavior of dioxan-water mixture with the micellar environment makes us easy to choose that mixture to study the micropolarity in the micellar media. A plot of emission maxima in dioxan-water mixtures vs $E_T(30)$ as represented in Figure 5, establishes a linear relationship between the parameters.

Assuming the same relationship also holds in the micellar media and comparing fluorescence maxima (λ_{max}^{em}) of PZ in different micelles such as SDS, CTAB and TX-100, the obtained

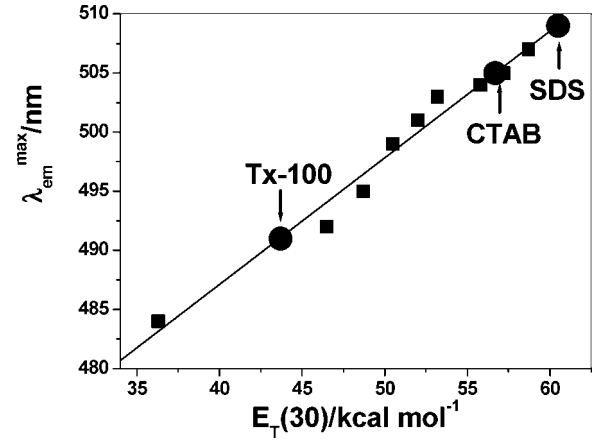

Figure 5. Variation of fluorescence maxima of PZ in dioxan−water mixed solvent and micellar media with E_T (30).

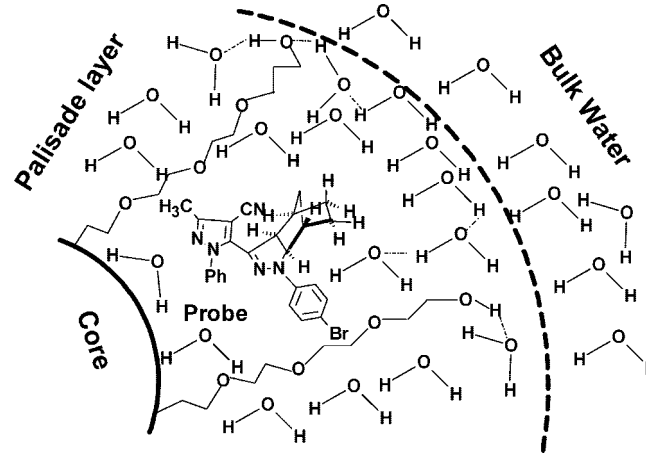

Figure 6. Qualitative picture of the palisade layer of TX-100 micelle. The probe PZ resides in the Palisade layer of the micelle.

TABLE 2: Recovered Decay Times (τ/ns) and Fraction of the Emitting Species in an Aqueous and Micellar Media

environments	α_1	τ_1/ns	α_2	τ_2/ns	χ^2
water	0.20	2.46	0.80	0.70	1.19
SDS (10 mM)	1.00	3.98			1.11
CTAB (2.5 mM)	1.00	5.13			1.35
TX-100 (1.4 mM)	1.00	6.32			1.18

$E_T(30)$ values (Table 1) are in agreement with the literature values.[52,53] Fluorescence quenching study and determination of micropolarity enables us to find the probable location of the fluorophore. The probe molecules may reside in Stern layer for ionic micelles and in the palisade layer for nonionic micelles (Figure 6).

Time-Resolved Fluorescence Measurement of Micelle-Bound Probe. Fluorescence lifetime serves as a sensitive indicator of the local environment in which a given fluorophore is placed.[54] Lifetime based measurement are rich in information and provide unique insights into the systems under investigation.[55] So modulated photophysics of this probe in micellar microenvironment compared to aqueous media has been demonstrated using time-resolved study (Table 2). In water and various micelles in the premicellar region, biexponential decay is observed. After the CMC in TX-100 a single exponential decay is observed whereas for ionic micelles biexponential curves are obtained but at the higher concentration of micelles single exponential curves are obtained (Figure 7).

Fluorescence quenching experiment has also been performed using this sensitive technique. The average fluorescence lifetime

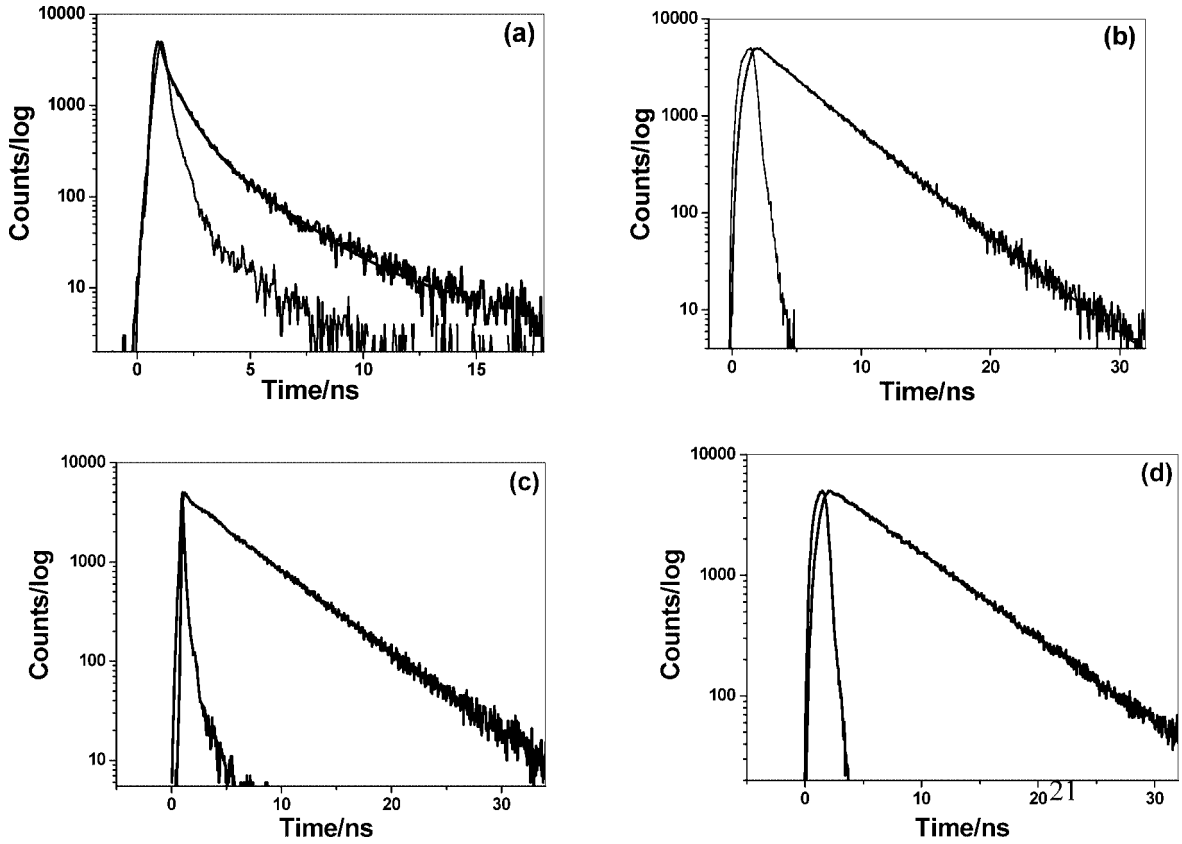

Figure 7. (a) Typical fluorescence decay curves associated with lamp profile for PZ in water. Biexponential fits are shown. Excitation wavelength is kept at 403 nm. (b) Typical fluorescence decay curves associated with lamp profile for PZ in SDS. Single exponential fits are shown. Excitation wavelength is kept at 403 nm. (c) Typical fluorescence decay curves associated with lamp profile for PZ in CTAB. Single exponential fits are shown. Excitation wavelength is kept at 403 nm. (d) Typical fluorescence decay curves associated with lamp profile for PZ in TX-100. Single exponential fits are shown. Excitation wavelength is kept at 403 nm.

TABLE 3: Recovered Decay Times (τ/ns) and Fraction of the Micelle Bound Emitting Species in Presence of Urea of Different Concentrations

micellar environment	[urea]/mol dm^{-3}	α_1	τ_1/ns	α_2	τ_2/ns	τ_{av}/ns	χ^2
SDS	4.0	0.07	2.61	0.93	3.85	3.76	1.25
	8.0	0.10	2.07	0.90	3.47	3.33	1.23
CTAB	2.0	1.00	5.04				1.21
	6.0	1.00	4.89				1.17
	8.0	0.23	2.32	0.77	5.14	4.49	1.27
TX-100	4.0	1.00	5.94				
	8.0	0.27	1.42	0.73	5.40	4.33	1.09

of a micelle bound probe decreases in presence of quencher CpCl. With increasing concentration of CpCl, decay at 496 nm becomes gradually faster with an average lifetime decreasing from 6.32 to 1.65 ns, 5.13 to 3.36 ns, and 3.98 to 3.29 ns in TX-100, CTAB and SDS micellar media, respectively, for varying concentrations of CpCl from 0.05 to 4.0 m mol dm^{-3}. The rate constant of quenching (k_q) of PZ fluorescence by CpCl quencher has been determined using the relation[29,56]

$$\frac{1}{\tau} = \frac{1}{\tau_0} + k_q[Q] \tag{6}$$

where τ and τ_0 are the lifetimes of PZ in presence and absence of quencher CpCl. The linearity of the plot $1/\tau$ vs [Q] indicates one type of quenching (inset of Figure 3). The quenching rate constants are presented in Table 1. The rate constant values obtained from steady state fluorescence measurement also (Table1) follow the same trend. Any change in the microenvironment of a micelle-bound probe therefore could be expected to give rise to variation in fluorescence lifetime. There is a continuous decrease in average lifetime (Table 3) of micelle bound probe with increasing urea concentration in the micelles.

All fluorescence decays for micelle bound PZ could be fitted well with a biexponential function at higher concentration of urea. This may be basically due to denaturation of micelle and reorientation of the probe molecule in two different sites. Thus the nature of the micelles (i.e., ionic or nonionic) also affects the quenching dynamics.

The change in lifetime value of PZ in presence of quencher further indicates the dynamic quenching of PZ and the dependence of quenching efficiency of quencher on micellar microenvironment surrounding the probe PZ. Lifetimes are shortened in a polar environment, which offers a convenient way to study micellar organization with varying concentration of urea. Three distinct regions are observed in a micelle, a nonpolar core formed by the hydrocarbon tail of the surfactant, a compact Stern layer having the head groups or palisade layer for nonionic micelle, and a wider Gouy–Chapman layer containing the counterions. A probe molecule may bind either to the headgroup

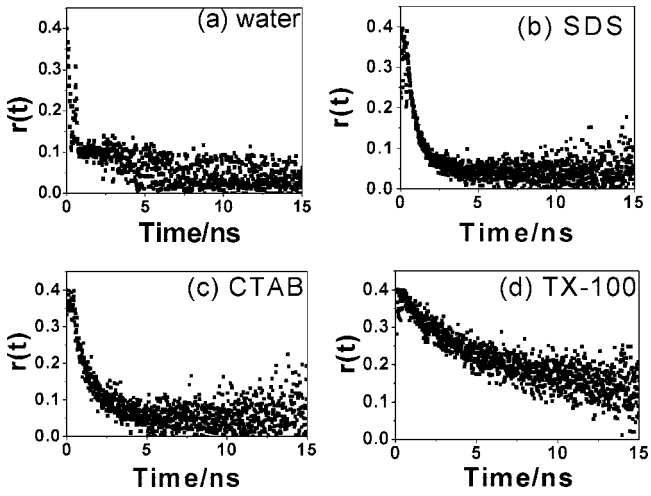

Figure 8. Typical time-resolved anisotropy decay for PZ in (a) water, (b) SDS, (c) CTAB and (d) TX-100. Excitation laser pulse is kept at 405 nm.

region or to the nonpolar core of the micelles. Depending on the nature of the solute, the solute molecules reside in any one of the sites. The Stern layer for ionic and palisade layer for nonionic micelles consists of polar head groups and largely structured water molecules. Single exponential fluorescence decay indicates that the fluorescent probe may exist either in a single environment or in different environments with rapid exchange between them on the time scale of measurements. Because the dioxan−water mixture resembles that of micellar phase, the lifetime of PZ in dioxan−water mixture has been determined. A single exponential curve has also been obtained in the mixture of more than 20% DX. The photophysical variation of PZ in aqueous solution, EG and GL from protic and aprotic solvents, dioxan-water mixture arises due to hydrogen bonding interaction with PZ.[20] In polar protic solvents the relaxation dynamics and steady state fluorescence depend not only on the polarity of the medium but also on specific interaction. In aqueous solution, ethylene glycol and glycerol media fluorescence from S_2 and S_1 states has been observed[20] but in micellar media, due to the strong micelle−PZ interaction (represented by binding constant values in Table 1) it may be assumed that S_1 state along the configuration coordinate crosses the S_2 potential surface in micellar medium resulting a high radiative relaxation from S_1 state. Hence no emission from S_2 state is observed here. The fluorescence quenching study also supports this assumption. An increase in the fluorescence lifetime in CTAB compared to SDS in ionic micelles may be due to the nature of the Stern layer for which binding constant of the probe with the micelles differ. In nonionic micelle TX-100, the lifetime of PZ is higher compared to ionic micelles. This can be ascribed to the additional stabilization of the probe as a result of the strong binding interaction with the TX-100 having thick palisade layer.

Time-Resolved Anisotropy. Time-resolved anisotropy is a sensitive way to determine the rotational relaxation of the probe in the micellar assembly.[29,57] To obtain incisive pertinent to the mobility of the probe molecule in these micellar systems, time-resolved anisotropy was performed. The fluorescence anisotropy decay of the probe in pure solvent is single exponential. In the case of micellar systems of SDS and CTAB (Figure 8) the decays are single exponential; the fluorescence depolarization is solely due to the rotational dynamics of a single fluorophore species encapsulated in the micelle. A single exponential function in TX-100 for $r(t)$ gave a poor fit to the data. However, a biexponential function for $r(t)$ was adequate to fit the data. The functional form of the anisotropy decay $r(t)$ is given by the following equation[29]

$$r(t) = r_0[\beta \exp(-t/\tau_{slow})] + (1-\beta)\exp(-t/\tau_{fast}) \quad (7)$$

where r_0 is the limiting anisotropy, which describes the inherent depolarization of the probe molecule. β is a pre-exponent, τ_{slow} and τ_{fast} are the two orientation times of the probe in the micelle. From various studies in the literature[58,59] it has been well established that the biexponential anisotropy decay of the probes observed in micellar systems is neither due to the fact that the probe is solubilized in two distinct regions of the micelle nor due to anisotropy rotation of the probe. The observed biexponential decay is due to the probe experiencing different kinds of rotation in micellar media. Such behavior is explained by using two-step model. According to this model,[60] probe molecule undergoes slow lateral diffusion on the spherical surface of the micelle and also fast wobbling motion in the micelle that are coupled to the rotation of the micelle as a whole. The probe used here is hydrophobic in nature where the lateral diffusion does not occur on the surface of the micelle, instead it takes place inside the micelle. The probe moves by exchanging position through interstitial sites. The experimentally measured τ_{slow} and τ_{fast} are used to calculate time constants for lateral diffusion τ_L, wobbling motion τ_W and overall rotation of the micelle τ_M by the relations

$$\frac{1}{\tau_{slow}} = \frac{1}{\tau_L} + \frac{1}{\tau_M} \quad (8)$$

$$\frac{1}{\tau_{fast}} = \frac{1}{\tau_W} + \frac{1}{\tau_{slow}} \quad (9)$$

The time constant τ_M can be calculated using the Stoke−Einstein−Debye relation (SED) hydrodynamic theory with the stick boundary condition[61]

$$\tau_M = \frac{\eta V_h}{kT} \quad (10)$$

where V_h is hydrodynamic volume of the micelle, η is the viscosity of the medium, and k and T are the Boltzmann constant and absolute temperature, respectively.

However, the central theme of this work, i.e. microviscosities, can be obtained from the average reorientation time under the assumption that $\langle\tau_r\rangle$ follows the SED relation.

$$\langle\tau_r\rangle = \beta\tau_{slow} + (1-\beta)\tau_{fast} \quad (11)$$

The average reorientation time due to the rotation of the probe in the micelle, $\langle\tau_r\rangle_P$ has been obtained using the following relation

$$\frac{1}{\langle\tau_r\rangle} = \frac{1}{\langle\tau_r\rangle_P} + \frac{1}{\tau_M}$$

Now, microviscosities (η_M) of the micelles can be obtained with the aid of the following SED relation

$$\eta_m = \frac{\langle\tau_r\rangle_P kT}{V_h} \quad (12)$$

where V_h, the hydrodynamic volume of the probe (here the value is 432 Å^3 for PZ), has been determined by the PM3 semiempirical calculation.

The η_M values reported in Table 4, however, correspond to that of the Stern layer of the ionic micelles and palisade layer of nonionic micelle.[64] Thus a study of different properties of

TABLE 4: Anisotropy Decay Parameters of PZ in Micelles, Hydrodynamic Radii, Reorientation Times and Microviscosities (Obtained from the Average Reorientation Times of PZ) of the Micelle (Rotational Time Scale of PZ in Water = 50 ps)

environment	τ_{slow}/ns	τ_{fast}/ns	r_M/Å	τ_M/ns[a]	η_m/mPa s
SDS	0.72		20.7[62]	8.3	7.5
CTAB	1.26		25.7[62]	15.4	13.1
TX-100	4.66	0.058	43.0[63]	72.0	27.4

the probe provides the same information regarding the local environment and excited state behaviors.

Conclusions

Photophysical properties of PZ with potential for applications in pharmaceutical industry were systematically studied in ionic and nonionic micelles. The fluorescence emission was found to be more media dependent compared to absorption. This has been exploited to determine the binding efficiency with micelles and nature of the microenvironment around the probe. The binding is, however, to a greater extent with nonionic micelle TX-100 rather than ionic micelles CTAB and SDS. The fluorophore molecules bound to different micelles are released to the bulk phase to different extent in presence of urea. Fluorescence quenching study indicates the location of the fluorophore in the micellar environment. Time-resolved study also reveals that the S_1 state is affected more in nonionic micellar environment than ionic micellar environments. Time-resolved anisotropy (single exponential for ionic micelles and biexponential for nonionic micelle) establishes the difference in rotational relaxation of the probe in different micellar assembly. The location of the probe is also ascertained from the order parameters, which is the Stern layer for ionic micelles and palisade layer for nonionic micelle. The probe sensing microviscosity in the micellar assembly has been estimated with the help of SED hydrodynamic theory from the average reorientation times.

Acknowledgment. Financial assistance from CSIR (01(2057)/06/EMR-II) is gratefully acknowledged. We acknowledge Dr. S. K. Pal, S. N. Bose National institute for Basic Sciences for his help with time correlated single photon counting (TCSPC) and Dr. S. Bhattacharya, University of Burdwan for the theoretical calculation.

Supporting Information Available: The sigmoidal curves for determination of CMC of representative micelles. This material is available free of charge via the Internet at http://pubs.acs.org.

References and Notes

(1) Roelfvan, S. G.; Arnold, C.; Wellnga, K. *J. Agric. Food Chem.* **1979**, *84*, 406.
(2) Goodell, J. R.; Puig-Basagoiti, F.; Forshey, B. M.; Shi, P.-Y.; Ferguson, D. M. *J. Med. Chem.* **2006**, *49*, 2127.
(3) Kedar, R. M.; Vidhale, N. N.; Chincholkar, M. M. *Orient. J. Chem.* **1997**, *13*, 143.
(4) Singh, A.; Rathod, S.; Berad, B. N.; Patil, S. D.; Dosh, A. G. *Orient. J. Chem.* **2000**, *16*, 315.
(5) Garge, H. G.; Chandraprakash, J. *Pharm. Sci.* **1971**, *14*, 649.
(6) Krishna, R.; Pande, B. R.; Bharthwal, S. P.; Parmar, S. S. *Eur. J. Med. Chem.* **1980**, *15*, 567.
(7) Kucukguzel, S. G.; Rollas, S. *Farmaco.* **2002**, *57*, 583.
(8) Jeong, T.-S.; Kim, K. S.; An, S.-J.; Cho, K.-H.; Lee, S.; Lee, W. S. *Bioorg. Med. Chem. Lett.* **2004**, *14*, 2715.
(9) Nakagawa, T.; Fujio, M.; Ozawa, T.; Minami, M.; Satoh, M. *Bihvioural Brain Res.* **2005**, *156*, 233.
(10) Xiao, D.; Xi, L.; Yang, W.; Fu, H.; Shuai, Z.; Fang, Y.; Yao, J. *J. Am. Chem. Soc.* **2003**, *125*, 6740.
(11) Barbera, J.; Clays, K.; Gimenez, R.; Houbrechts, S.; Persoons, A.; Serrano, J. L. *J. Mater. Chem.* **1998**, *8*, 1725.
(12) Fu, H.; Xiao, D.; Yao, J.; Yang, G. *Angrew. Chem. Int. Ed.* **2003**, *42*, 2883.
(13) Oh, S. W.; Zhang, D. R.; Kang, Y. S. *Mater. Sci. Eng.* **2004**, *24*, 131.
(14) Yin, J. S.; Wang, Z. L. *Phys. Rev. Lett.* **1997**, *79*, 2570.
(15) Fu, H.-B.; Xie, R.-M.; Wang, Y.-Q.; Yao, J.-N. *Col. Surf. A: Phys. Eng. Asp.* **2000**, *174*, 367.
(16) Silinsh, E. A. *Organic Molecular Crystals: Their Electronic States*; Springer-Verlag: Berlin, 1980.
(17) Rurack, K.; Bricks, J. L.; Schulz, B.; Maus, M.; Reck, G.; Resch-Genger, U. *J. Phys. Chem. A* **2000**, *104*, 6171.
(18) Fahrni, C. J.; Yang, L.; Van Derveer, D. G. *J. Am. Chem. Soc.* **2003**, *125*, 3799.
(19) Zhang, L.; Zhang, B.; Cao, Y. *Acta Phys.-Chem. Sinica* **1999**, *15*, 917.
(20) Chatterjee, S.; Banerjee, P.; Pramanik, S.; Mukherjee, A.; Mahalanabis, K. K.; Bhattacharya, S. C. *Chem. Phys. Lett.* **2007**, *440*, 313.
(21) Karmakar, R.; Samanta, A. *Chem. Phys. Lett.* **2003**, *376*, 638.
(22) Mallick, A.; Haldar, B.; Maiti, S.; Bera, S. C.; Chattopadhyay, N. *J. Phys. Chem. B* **2005**, *109*, 14675.
(23) Tanford, C. *Science* **1978**, *200*, 1012.
(24) Tanford, C. *The Hydrophobic Effect; Formation of micelles and Biological Membranes*; Wiely-Interface: New York, 1980.
(25) Kimizuka, N.; Wakiyama, T.; Miyauchi, H.; Yoshimi, T.; Tokuhiro, M.; Kunitake, T. *J. Am. Chem. Soc.* **1996**, *118*, 5808.
(26) John, A.; Vreeland, W. N.; DeVoe, D. L.; Locascio, L. E.; Gaitan, M. *Langmuir* **2007**, *23*, 6289.
(27) Attwood, D. *Microemulsion. In Colloid Drug Delivery Systems*; Kreuter, J., Ed.; Marcel Dekker: New York, 1994.
(28) Alkan-Oxynksel, H.; Ramkrishnan, S.; Chai, H. B.; Pazzuto, J. M .*Pharm. Res.* **1994**, *11*, 206.
(29) Lakowicz, J. R. *Principles of Fluorescence Spectroscopy*; Kluwer-Plenum Press: New York, 1999.
(30) Bhattacharyya, K.; Chowdhury, M. *Chem. Rev.* **1993**, *93*, 507.
(31) Shannigrahi, M.; Bagchi, S. *J. Photochem. Photobiol. A: Chem.* **2004**, *168*, 133.
(32) Behera, G. B.; Mishra, B. K.; Behera, P. K.; Panda, M. *Adv. Colloid Interface Sci.* **1999**, *82*, 1.
(33) Kalyanasundaram, K. *Photochemistry in Microheterogeneous Systems*; Academic Press: New York, 1991.
(34) Majhi, P. R.; Moulik, S. P. *Langmuir* **1998**, *14*, 3986.
(35) Jones, M. N.; Chapman, D. *Micelles, Monolayers and Biomembranes*; Wiley-Liss: New York, 1995.
(36) Almgren, M.; Grieser, F.; Thomas, J. K. *J. Am. Chem. Soc.* **1979**, *101*, 279.
(37) Turro, N. J.; Yekta, A. *J. Am. Chem. Soc.* **1978**, *100*, 5951.
(38) Saroja, G.; Ramachandram, B.; Saha, S.; Samanta, A. *J. Phys. Chem. B* **1999**, *103*, 2906.
(39) Kumbhakar, M.; Goel, T.; Mukherjee, T.; Pal, H. *J. Phys. Chem. B* **2004**, *108*, 19246.
(40) Shannigrahi, M.; Bagchi, S. *J. Phys. Chem. B* **2004**, *108*, 17703.
(41) Hansson, P.; Almgren, M. *J. Phys. Chem B* **2000**, *104*, 1137.
(42) Komaromy-Hiller, G.; Calkins, N.; von Wandruszka, R. *Langmuir* **1996**, *12*, 916.
(43) Bhattacharya, S. C.; Das, H. T.; Moulik, S. P. *J. Photochem. Photobiol A: Chem.* **1993**, *71*, 257.
(44) Finer, E. G.; Franks, F.; Tait, M. J. *J. Am. Chem. Soc.* **1972**, *94*, 4424.
(45) Ruiz, C. C.; Sanchez, F. G. *J. Colliod. Interface. Sci.* **1994**, *165*, 110.
(46) Roseman, M.; Jencks, W. P. *J. Am. Chem. Soc.* **1975**, *97*, 631.
(47) Christianziana, P.; Lelj, F.; Amodeo, P.; Barone, G.; Barone, V. *J. Chem. Soc., Faraday Trans 2* **1989**, *5*, 621.
(48) Muller, N. In *Reaction Kinetics in Micelles*; Cordes, E. A., Ed.; Plenum: New York, 1973.
(49) Kalyanasundaram, K.; Thomas, J. K .*J. Am. Chem. Soc.* **1977**, *99*, 2039.
(50) Mallick, A.; Haldar, B.; Maiti, S.; Chattopadhyay, N. *J. Colloid Interface Sci.* **2004**, *278*, 215.
(51) Kosower, E. M.; Dodiuk, H.; Tanizawa, K.; Ottolenghi, M.; Orbach, N. *J. Am. Chem. Soc.* **1975**, *97*, 2167.
(52) Saroja, G.; Samanta, A. *Chem. Phys. Lett.* **1995**, *246*, 506.
(53) Kalyanasundaram, K.; Thomas, J. K. *J. Phys. Chem.* **1977**, *81*, 2176.
(54) Maciejewski, A.; Demmer, D. R.; James, D. R.; Safarzadeh-Amiri, A.; Verrall, R. E.; Steer, R. P. *J. Am. Chem. Soc.* **1985**, *107*, 2831.
(55) Bright, F. V.; Munson, C. A. *Anal. Chim. Acta* **2003**, *500*, 71.
(56) Roy, D.; Karmakar, R.; Mondal, S. K.; Sahu, K.; Bhattacharyya, K. *Chem. Phys. Lett.* **2004**, *399*, 147.

(57) Fleming, G. R. In *Chemical applications of Ultrafast Spectroscopy*; Oxford University Press: New York, 1986.
(58) Quitevis, E. L.; Marcus, A. H.; Fayer, M. D. *J. Phys. Chem.* **1993**, *97*, 5762.
(59) Dutt, G. B. *J. Phys. Chem. B* **2003**, *107*, 10546.
(60) Lipari, G.; Szabo, A. *J. Am. Chem. Soc.* **1982**, *104*, 4546.
(61) Debye, P. *Polar Molecules*; Dover: New York, 1929.
(62) Maiti, N. C.; Krishna, M. M. G.; Britto, P. J.; Periasamy, N. *J. Phys. Chem. B* **1997**, *101*, 11051.
(63) Robson, R. J.; Dennis, E. A. *J. Phys. Chem.* **1977**, *81*, 1075.
(64) Dutt, G. B. *J. Phys. Chem. B* **2004**, *108*, 3651.

JP800200V